



1 **Ammonium and nitrite oxidation in the upper euphotic zone of the oligotrophic Red Sea**

2 Eyal Rahav^{1,2,3*}, Scott D Wankel⁴, and Adina Paytan²

3

4 ¹ Israel Oceanographic and Limnological Research, Haifa, Israel.

5 ² Institute of Marine Science, University of California, Santa Cruz, CA, USA.

6 ³ Department of Earth and Environmental Science, Ben-Gurion University of the Negev, Beer
7 Sheva, Israel.

8 ⁴ Marine Chemistry and Geochemistry Department, Woods Hole Oceanographic Institution,
9 Woods Hole, Massachusetts, USA.

10

11 *Corresponding author: eyrahav@ucsc.edu; eyal.rahav@ocean.org.il

12

13 **Abstract**

14 Nitrification is widely understood to be inhibited by light in the surface ocean, however,
15 increasing evidence indicates its occurrence at low levels at many sites. The extent to which
16 nitrification remains active in the euphotic zone could have important implications to new
17 production calculations, yet it remains understudied. Here, we quantified ammonium and nitrite
18 oxidation rates in the euphotic zone of the Gulf of Aqaba (Northern Red Sea) from late spring
19 to late summer and examined environmental controls and implications for dark carbon fixation
20 (chemoautotrophy) and new production. Both ammonium and nitrite oxidation were detectable
21 throughout the euphotic zone (~ 0.1 - 0.8 nmol N L⁻¹ d⁻¹). Overall, rates increased with depth and
22 were strongly suppressed in the highest irradiance surface waters. Integrated rates over the
23 entire euphotic zone (24 - 56 μ mol N m⁻² d⁻¹) were among the lowest reported for oligotrophic
24 regions globally. This reflects extremely low substrate concentrations and intense, though not
25 complete, photoinhibition. Ammonium and nitrite oxidation together supported <2% of
26 chemoautotrophic activity, suggesting other processes, not accounted for, such as anaplerosis
27 may be important. Depth-resolved correlations with environmental parameters highlight light,
28 temperature, and substrate availability as key regulators of both processes. Our results show
29 that nitrification in the Gulf of Aqaba operates at the lower bounds of global euphotic zone
30 rates and is loosely coupled to carbon cycling. These findings underscore the need to better
31 resolve nitrification dynamics in ultra-oligotrophic, rapidly warming, seas to refine estimates
32 of new production and chemoautotrophic carbon assimilation under future ocean conditions.



33

34 **Key words:** Ammonia oxidation, Nitrite oxidation, Dark carbon fixation, Red Sea,
35 Oligotrophic.

36

37 **1 Introduction**

38 Nitrification, the sequential oxidation of ammonium (NH_4^+) to nitrite (NO_2^-) followed
39 by the oxidation of nitrite to nitrate (NO_3^-), is a microbially mediated process central to the
40 regulation of nitrogen availability across nearly all aquatic environments, linking the most
41 reduced and oxidized states of nitrogen (Ward, 2008). Although nitrification does not change
42 the absolute inventory of bioavailable nitrogen (N) in the oceans, it alters the balance among
43 N species that serve as substrates for different organisms, thereby affecting phytoplankton
44 species abundance and growth (Fawcett et al., 2011). Ammonia oxidation is carried out by
45 ammonia-oxidizing archaea and bacteria (Francis et al., 2005; Wuchter et al., 2006), while
46 nitrite oxidation is performed by nitrite-oxidizing bacteria (Mincer et al., 2007; Pachiadaki et
47 al., 2017). Ammonia-oxidizing bacteria that perform the entire process have also been
48 identified in freshwater, terrestrial, and coastal habitats, but have not yet been found in the open
49 ocean (Daims et al., 2015; Fei et al., 2018; van Kessel et al., 2015).

50 Nitrification has been investigated across a wide range of marine settings, including the
51 Atlantic (Clark et al., 2008, 2022), the Pacific (Wan et al., 2021; Wankel et al., 2007), and the
52 Polar (Mdutyana et al., 2020; Shiozaki et al., 2019) ocean basins, as well as numerous coastal
53 and estuarine systems (Henriksen and Kemp, 1988; Herbert, 1999; Zhu et al., 2018). As a
54 chemoautotrophic process, nitrification contributes to organic carbon production in the ocean
55 interior (Middelburg, 2011; Pachiadaki et al., 2017), and may fuel bacterial carbon demand and
56 support heterotrophic food-webs in the mesopelagic and bathypelagic water depths (Bayer et
57 al., 2024). The activity of nitrifiers is known to be promoted or inhibited by many
58 environmental factors (Ward, 2008), yet specific controls on its occurrence in the water column
59 and broader ecological implications across different ocean settings remain poorly constrained
60 (Tang et al., 2023). Additionally, because uptake of NH_4^+ and NO_3^- has long served to
61 differentiate between ‘regenerated’ and ‘new’ production, respectively (Eppley and Peterson,
62 1979), *in situ* production of NO_3^- by nitrification in the photic zone skews global estimates of
63 new production and carbon export in the oceans (Yool et al., 2007; Wankel et al., 2007).

64 Here, we report ammonium and nitrite oxidation rates in the euphotic zone (surface and
65 down to ~100 m) of the Gulf of Aqaba (GoA, Northern Red Sea) during late spring and



66 throughout the summer season. Rates were compared with common environmental
67 physiochemical and biological parameters to assess drivers of nitrification in this setting. Using
68 these data, we provide estimates of the contribution of ammonium and nitrite oxidation to dark
69 carbon fixation (DCF) and new production in this oligotrophic, warm and well-lit system.

70 **2 Material and methods**

71 Seawater was collected every 20 m throughout the euphotic zone (0-100 m depth) at an
72 offshore, routinely monitored, station in the GoA (“Station A”, latitude 29.47 N, longitude
73 34.92 E). Ammonium and nitrite oxidation rates were assessed using stable ^{15}N isotope
74 enrichment incubations. Five monthly sampling events were performed spanning late
75 spring/early summer (May) to late summer (September) in 2023, covering the period in which
76 the GoA is characterized by oligotrophic N-poor conditions (Fuller et al., 2005; Mackey et al.,
77 2007). Ancillary water column measurements included temperature, salinity, photosynthetic
78 active radiation (PAR) (Seabird 19 Plus), inorganic nitrogen species concentrations (NO_2^- ,
79 NO_3^- , NH_4^+), chlorophyll-*a*, and rates of photosynthesis and dark inorganic carbon fixation
80 (DCF).

81 **2.1 Inorganic nitrogen species**

82 Duplicate water samples for nitrite (NO_2^-) and nitrate (NO_3^-) were collected in 15 ml acid-clean
83 polyethylene tubes directly from Niskin bottles. Prior to filling, the tube was thoroughly rinsed
84 three times with sample water. After collection, samples were stored at 4 °C in the dark and
85 analyzed the following day. Nitrite (NO_2^-) and nitrate (NO_3^-) concentrations were determined
86 colorimetrically following standard procedures (Grasshoff et al., 1999). Nitrite was measured
87 directly using the Griess reaction, in which nitrite forms an azo dye after reaction with
88 sulfanilamide and N-(1-naphthyl)ethylenediamine and is quantified spectrophotometrically
89 ($\lambda=520$ nm). Nitrate was reduced to nitrite using a copper-coated cadmium reduction column
90 and subsequently nitrate + nitrite was analyzed by the same azo-dye method. Nitrate
91 concentrations were then calculated by difference. Analyses were performed using a Flow
92 Injection Autoanalyzer system (FIA, Lachat Instruments (Model QuikChem 8000)). The
93 analysis was automated, and peak areas were calibrated using standards prepared in nutrient-
94 deplete 0.2- μm filtered surface seawater from the GoA over a range of 0-100 nmol L^{-1} . The
95 detection limits were 10 nmol L^{-1} and 20 nmol L^{-1} for nitrite and nitrate, respectively, with
96 typical analytical precision of ~ 20 nmol L^{-1} , consistent with previous measurements in the GoA
97 (e.g., Mackey et al., 2011).



98 Samples for ammonium (NH_4^+) concentration were collected directly from Niskin bottles into
99 acid-washed plastic vials after rinsing 3 times with sample water. The collected samples were
100 stored in 4 °C in the dark and analyzed within an hour after collection. Ammonium
101 concentrations were determined using the orthophthaldialdehyde (OPA) method (Holmes et al.,
102 1999), where samples were first incubated with a working reagent of OPA for 3 h and then
103 measured fluorometrically (Turner Designs, Ex: 360 nm, Em. 420 nm). The detection limit of
104 the OPA analysis was $\sim 4 \text{ nmol L}^{-1}$ (Meeder et al., 2012).

105 2.2 Ammonium and nitrite oxidation rates

106 Ammonium and nitrite oxidation rates were determined using stable isotope tracer incubations
107 (Beman et al., 2011; Bristow et al., 2015; Ward, 1987). Seawater was collected into triplicate
108 0.5-L acid-cleaned transparent Nalgene bottles without headspace. The bottles were incubated
109 on land for 24 h in aquarium tanks continuously supplied with running surface seawater, using
110 neutral density screening nets simulating the light conditions of the collection depth (no change
111 in spectra). For ammonia oxidation, samples were amended with ^{15}N -labeled ammonium
112 chloride ($^{15}\text{NH}_4\text{Cl}$, >98 atom %; Cambridge Isotope Laboratories) at a concentration of ~ 20
113 nmol L^{-1} which was expected to provide a quantifiable signal without substantially enhancing
114 oxidation rates. For nitrite oxidation, samples were amended with $\sim 5 \text{ nmol L}^{-1}$ of ^{15}N -labeled
115 sodium nitrite ($^{15}\text{NO}_2^-$, >98 atom %), again minimally perturbing the *in situ* nitrite pool. At the
116 end of the incubation, subsamples were filtered onto a Supor 0.22 μm (47 mm) filter using
117 gentle filtration, and the filtrate ($< 0.22 \mu\text{m}$) was kept frozen in the dark at $-20 \text{ }^\circ\text{C}$ until analysis.
118 For ammonia oxidation, the presence of $^{15}\text{NO}_2^-$ in the total dissolved nitrite pool was quantified
119 by isotope ratio mass spectrometry (IRMS) after chemical conversion to N_2O using the azide
120 method (McIlvin and Altabet, 2005). For nitrite oxidation, we quantified the $^{15}\text{NO}_3^-$ in the
121 dissolved nitrate pool after conversion to nitrous oxide via the denitrifier method (Sigman et
122 al., 2001) and subsequent IRMS analysis. Additionally, killed controls poisoned with HgCl_2
123 from each collection depth were incubated in parallel to account for any abiotic transformations
124 and subtracted from the ‘live’ bottles. Rates in the ‘mercury-killed’ controls were typically
125 negligible relative to the ‘live’ bottles. Rates of ammonium and nitrite oxidation were
126 calculated following previous studies (Beman et al., 2011; Bristow et al., 2015; Ward, 1987) as
127 shown in in Eq. 1-3:

128

$$129 \quad (1) \text{ Ammonia oxidation} = \frac{\Delta (\text{atm\% } ^{15}\text{N NO}_2) \times [\text{NO}_2]_{\text{final}}}{t \times F (\text{NH}_4)}$$

130



131 (2) Nitrite oxidation = $\frac{\Delta(\text{atm}\% \text{ } ^{15}\text{N NO}_3^-) \times [\text{NO}_3^-]_{\text{final}}}{t \times F(\text{NO}_2)}$

132

133 (3) F substrate = $\frac{[^{15}\text{N substrate}]_{\text{added}}}{[\text{Substrate ambient}] + [\text{Substrate added}]}$

134

135 Where, $\Delta(\text{atm}\% \text{ } ^{15}\text{N NO}_2^-)$ or $\Delta(\text{atm}\% \text{ } ^{15}\text{N NO}_3^-)$ = atom% excess ^{15}N in the nitrite or nitrate
136 pool relative to natural abundance; $[\text{NO}_2^-]_{\text{final}}$ or $[\text{NO}_3^-]_{\text{final}}$ = final concentration of the nitrite
137 or nitrate pool (nmol L^{-1}); t = time (d); F_{NH_4} or F_{NO_2} = fractional ^{15}N enrichment of the
138 ammonium or nitrite substrate pool.

139

140 2.3 Photosynthesis and Dark Carbon Fixation (DCF)

141 Photosynthesis and chemoautotrophic DCF rates were measured using $\text{NaH}^{14}\text{CO}_3$
142 incorporation method (Steemann-Nielsen, 1952) with minor modifications (Reich et al., 2024,
143 2026). Triplicate seawater samples were collected from Niskin bottles in 50 ml acid-washed
144 falcon tubes and spiked with a diluted ‘working solution’ of $\text{NaH}^{14}\text{CO}_3$ (Perkin Elmer, specific
145 activity 56 mCi mmol^{-1}) at a final radioisotope dilution of 1:10⁴ v:v. Tubes were incubated in
146 the same tanks and under the same conditions used for the ammonium and nitrite oxidation
147 measurements with one exception – the DCF bottles were first covered with aluminum foil to
148 prevent light penetration. The tubes were incubated for 24 h before being filtered onto GF/F
149 filters (0.7 μm nominal pore size, 25 mm diameter) using low vacuum pressure (<50 mmHg).
150 The filters were placed in glass scintillation vials and 50 μl of 37% hydrochloric acid was added
151 to remove the non-fixed ^{14}C -bicarbonate overnight. Scintillation cocktail (5 ml, ULTIMA-
152 GOLD) was then added to each vial and samples were counted using a TRI-CARB 4810 TR
153 (Packard) liquid scintillation counter. Additional T_0 blanks were prepared by spiking bottles
154 with $\text{NaH}^{14}\text{CO}_3$ and filtering immediately (without incubation). Blanks consistently yielded
155 negligible activity. Added activity was measured by withdrawing 50 μl from representative
156 spiked bottles (immediately after dosing and before incubation) and adding it onto a new GF/F
157 filter with 50 μl of ethanolamine ($\text{pH} \approx 12$) followed by scintillation cocktail and counting
158 immediately.

159 Photosynthesis was calculated as the difference between the disintegration per minute (DPM)
160 measured in the samples incubated under ambient irradiance and the dark bottles. DCF and
161 photosynthesis rates were calculated based on the Bermuda Atlantic Time-series Study (BATS)
162 protocol using the following Eq. 4:



163 (4) $Production = \frac{(DPM-blank)}{V} \times DIC \times \frac{AA\ vol}{TDPM} \times f \times \frac{1}{t}$

164 Where, DPM equals the disintegrations per minute, V = the filtered volume (50 ml), DIC is the
165 dissolved inorganic carbon in seawater (~25 mg C L⁻¹, similar to other oceanic sites, (Knap and
166 Michaels, 1993), AA vol = Added activity volume (50 µl), TDPM = Total ¹⁴C disintegration
167 per minute, t = incubation time (24h), and f = factor correcting isotope fractionation during
168 uptake of ¹⁴C (1.05).

169

170 2.4 Chlorophyll.a analysis

171 Seawater samples (250 ml) were filtered onto Whatman GF/F filters at low pressure (<150
172 mbar), placed in glass vials and frozen in the dark at -20 °C. Chlorophyll.a was extracted with
173 5 ml of cold acetone (90 %) overnight and determined by the non-acidification method
174 (Welschmeyer, 1994) using a Turner Designs (Trilogy) fluorometer.

175

176 3 Results and discussion

177 3.1 Physiochemical and biological characteristics of the GoA during summertime

178 Sampling spanned from late spring (May) to the end of summer (September) within the
179 euphotic zone (0-100 m) of the GoA. Surface temperatures ranged from ~25 °C in May to ~28
180 °C at the end of summer (September) and declined to ~23.5 °C at 100 m during all sampling
181 events (Figure 1A). Photosynthetic active radiation (PAR) levels ranged from ~1200-1950
182 µmol quanta m⁻² s⁻¹ at the surface and decreased exponentially to ~10-20 µmol quanta m⁻² s⁻¹
183 at 100 m (Figure 1B), corresponding to 0.5-2% of the surface irradiation levels. The
184 corresponding diffuse attenuation coefficient (Kd) was ~0.03-0.04 m⁻¹, in agreement with
185 previous observations from the GoA (Dishon et al., 2012; Stambler, 2006) and other
186 oligotrophic regimes (Stambler, 2012). Concentrations of NH₄⁺ ranged from undetectable to
187 65 nmol L⁻¹ without a clear vertical or temporal trend, except in May where surface
188 concentrations were below detection (Figure 1C). The corresponding integrated NH₄⁺
189 inventory (0-100 m) was lowest in May (1.68 µmol m⁻²) and highest in July (~4.57 µmol m⁻²)
190 (Table 1). NO₂⁻ levels were generally low throughout the upper 100 m (from below detection
191 to <20 nmol L⁻¹), except in September when nitrite increased with depth reaching ~45 nmol L⁻¹
192 below 40 m (Figure 1D). Vertical NO₂⁻ profiles suggest active ammonia oxidation below the
193 strongly lit surface waters, especially during September, although we cannot rule out expulsion
194 of NO₂⁻ by phytoplankton under light limitation (Ko et al., 2022). Nevertheless, vertically



195 integrated NO_2^- inventories were generally low in all months examined, ranging from 0.79-
196 3.39 $\mu\text{mol m}^{-2}$ (Table 1). Surface NO_3^- was also low ($<20 \text{ nmol L}^{-1}$) and generally increased
197 with depth, suggesting organic matter regeneration and nitrification during summertime
198 (Figure 1E), and/or that less NO_3^- is assimilated by phytoplankton at deeper depths. The
199 integrated NO_3^- inventory ranged from 2.65 $\mu\text{mol m}^{-2}$ in May and September up to 10.36 μmol
200 m^{-2} in June (Table 1). Taken together, the summertime inorganic N species concentrations in
201 the upper 100 m were low, in agreement with previous reports from the oligotrophic GoA
202 (Mackey et al., 2011; Meeder et al., 2012; Rahav et al., 2015). The general increasing trend in
203 NO_2^- and NO_3^- with depth and the nano-molar NH_4^+ levels suggest active nitrification below
204 the well-lit surface water that has not been previously quantified in the GoA.

205 Phytoplankton biomass derived from chlorophyll.*a* was low in the surface water (<0.15
206 $\mu\text{g L}^{-1}$) and gradually increased with depth reaching maximal values in May and June (~ 0.60
207 $\mu\text{g L}^{-1}$) (Figure 2A). The corresponding integrated chlorophyll.*a* was 26-28 mg m^{-2} except in
208 August where it was 16 mg m^{-2} (Table 1). As expected, photosynthesis rates were highest in
209 the surface water and decreased with depth (Figure 2B), coinciding with the decreasing PAR
210 levels (Figure 1B). Photosynthesis rates decreased from $\sim 10 \mu\text{g C L}^{-1} \text{ d}^{-1}$ at the surface to below
211 detection at 100 m, except in September when elevated rates were observed throughout the
212 water column, ranging from ~ 10 to 25 $\mu\text{g C L}^{-1} \text{ d}^{-1}$ (Figure 2B). The resulting integrated
213 photosynthesis rates ranged from 242 $\text{mg C m}^{-2} \text{ d}^{-1}$ in August to as high as 1263 $\text{mg C m}^{-2} \text{ d}^{-1}$
214 in September (Table 1). Despite the fluctuation in photosynthetic rates between months, these
215 values are within the range previously reported from the GoA (Rahav et al., 2015; Reich et al.,
216 2024; Suggett et al., 2009).

217 Chemoautotrophic DCF was lower than photosynthesis rates and exhibited no clear
218 vertical trends (Figure 2C). The surface DCF ranged from ~ 0.2 - $0.6 \mu\text{g C L}^{-1} \text{ d}^{-1}$ to ~ 0.1 - $0.9 \mu\text{g}$
219 $\text{C L}^{-1} \text{ d}^{-1}$ at 100 m (Figure 2C). The resulting integrated DCF ranged from 17-37 $\text{mg C m}^{-2} \text{ d}^{-1}$,
220 in agreement with a recent study from the GoA (Reich et al., 2024), corresponding to ~ 3 -10%
221 of all the total autotrophic activity (photosynthesis + DCF). While multiple microbial
222 metabolisms involve chemoautotrophic carbon fixation, DCF is primarily attributed to
223 ammonium and nitrite oxidation, as these chemoautotrophic metabolisms are ubiquitous
224 throughout the oxic water column (Middelburg, 2011; Tang et al., 2023). In general, ammonia
225 oxidation likely provides energy that supports chemoautotrophic CO_2 assimilation throughout
226 the euphotic zone. Though less energy efficient, nitrite oxidation also contributes to DCF and
227 is considered especially relevant near the base of the euphotic zone where NO_2^- often
228 accumulates and reaches a maximum in concentration (Tang et al., 2023).



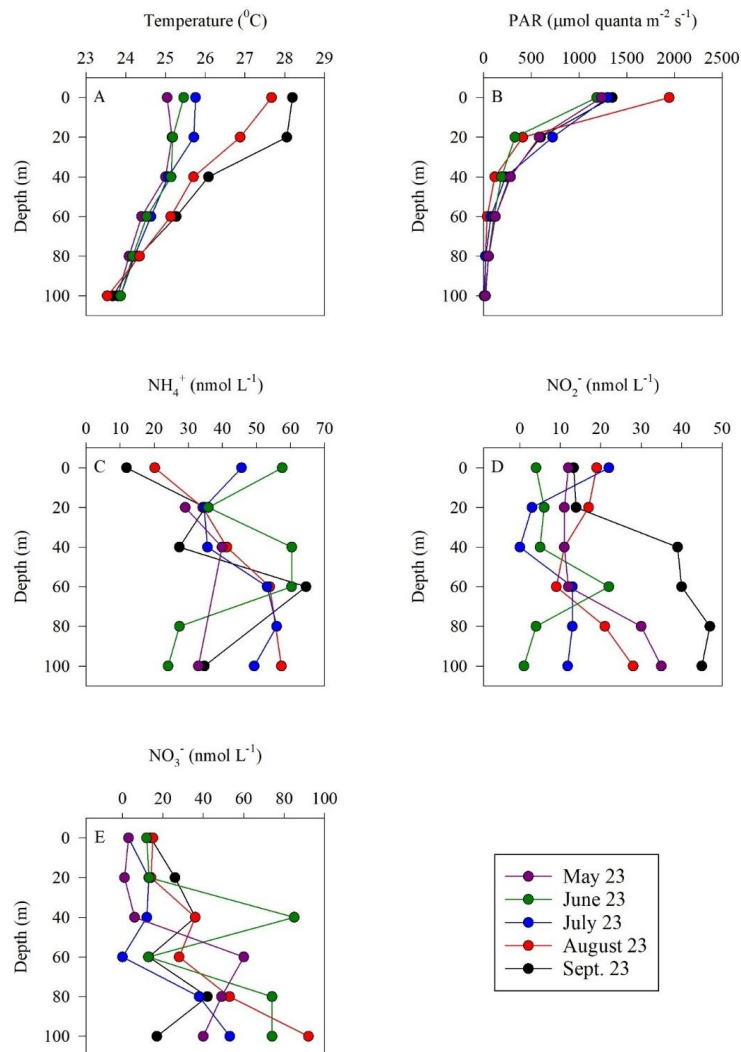
229 **Table 1:** Summary of integrated values (0-100 m) measured in the GoA (N Red Sea) during
 230 summer 2023.

Variable	May 23	June 23	July 23	Aug. 23	Sept. 23
NH ₄ ⁺ (μmol m ⁻²)	1.68	4.54	4.57	3.36	2.99
NO ₂ ⁻ (μmol m ⁻²)	1.76	0.79	0.94	1.64	3.39
NO ₃ ⁻ (μmol m ⁻²)	2.76	10.36	6.60	6.13	2.65
Chlorophyll. <i>a</i> (mg m ⁻²)	26	28	26	16	28
Photosynthesis (mg C m ⁻² d ⁻¹)	350	349	302	242	1263
DCF (mg C m ⁻² d ⁻¹)	32	17	35	27	37
NH ₄ ⁺ oxidation (μmol m ⁻² d ⁻¹)	28	48	39	45	56
NO ₂ ⁻ oxidation (μmol m ⁻² d ⁻¹)	24	38	45	39	44
Contribution of NH ₄ ⁺ oxidation to DCF (%)*	0.32	1.02	0.40	0.60	0.54
Contribution of NO ₂ ⁻ oxidation to DCF (%)**	0.05	0.13	0.08	0.09	0.07

231 *Assuming 0.3 moles of C fixed per mole of NH₄⁺ oxidized (Santoro et al., 2010).

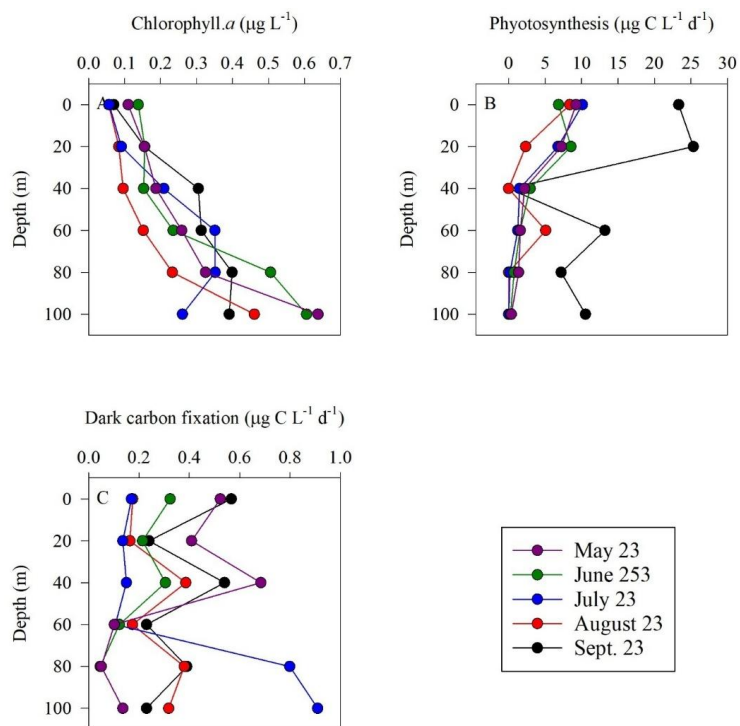
232 **Assuming 0.05 moles of C per mole of NO₂⁻ oxidized (Beman et al., 2013).

233



234

235 **Figure 1:** Vertical distribution of temperature (A), PAR (B), NH_4^+ (C), NO_2^- (D) and NO_3^- (E)
236 in the upper euphotic zone in the GoA, N Red Sea between May and September 2023.



237

238 **Figure 2:** Vertical distribution of chlorophyll-a (A), photosynthesis (B), and dark carbon
 239 fixation (C) in the upper euphotic zone in the GoA, N Red Sea between May and September
 240 2023.

241

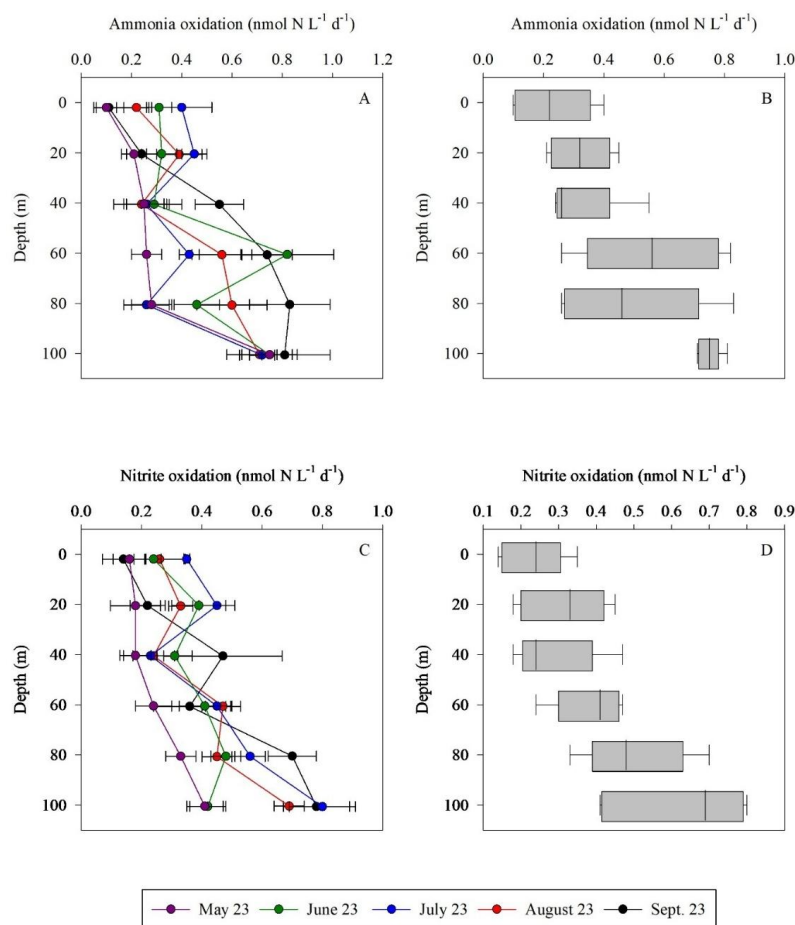
242 3.2 Ammonia and nitrite oxidation rates

243 Ammonia and nitrite oxidation rates were generally low throughout the euphotic zone
 244 yet exhibited an increasing trend with depth (Figure 3), consistent with regulation by light
 245 inhibition. Overall, ammonia oxidation was homogeneous in the upper 40 m, ranging from
 246 ~ 0.10 - $0.55 \text{ nmol N L}^{-1} \text{ d}^{-1}$. Below this depth rates increased towards the bottom of the euphotic
 247 zone ($\sim 100 \text{ m}$), ranging from ~ 0.26 - $0.83 \text{ nmol N L}^{-1} \text{ d}^{-1}$ (Figure 3A,B). Ammonia oxidation
 248 rates often reached a maximum near the base of the euphotic zone (below the 50-100 m layer)
 249 as seen in other studies (Tang et al., 2023). In general, these low euphotic zone ammonia
 250 oxidation rates are consistent with light inhibition, given the high PAR of the GoA during
 251 summer (Figure 1B, Wan et al., 2021). Competition of nitrifiers with phytoplankton for NH_4^+
 252 may also result in low ammonia oxidation rates, as has been reported in the surface sunlit North
 253 Pacific (Smith et al., 2014). However, the highest integrated ammonia oxidation rate
 254 (September, $56 \text{ } \mu\text{mol m}^{-2} \text{ d}^{-1}$) was measured when chlorophyll.a levels and primary



255 productivity were also relatively high and similar to springtime when the lowest ammonia
256 oxidation rates were measured (May, $28 \mu\text{mol m}^{-2} \text{d}^{-1}$) (Table 1). Thus, competition between
257 nitrifiers and phytoplankton for NH_4^+ does not appear to play a direct role in the regulation of
258 oxidation rates in our study. This is further supported by the lack of correlation between
259 chlorophyll.*a* and ammonium ($r^2 = 0.003$). Ammonia oxidation rates have also been shown to
260 be influenced by trace metal availability, specifically iron and copper (Martocello and Wankel,
261 2024; Shafiee et al., 2019, 2021). However, given the close proximity to major deserts, iron is
262 not considered a limiting factor for microbes in the surface water of the GoA (Chen et al., 2008;
263 Torfstein et al., 2017). The limiting factors for ammonia oxidizers in the GoA should be further
264 studied by simulating different nutrients and temperature scenarios with or without
265 amendments of an inhibitor of ammonia monooxygenase to better examine controls on
266 environmental rates (Bayer et al., 2024).

267 As with ammonia oxidation, rates of nitrite oxidation also increased with depth (Figure
268 3C,D). Nitrite oxidation ranged from 0.14 to $0.70 \text{ nmol L}^{-1} \text{d}^{-1}$ (Figure 3C,D), with highest rates
269 measured over 80-100 m. Integrated nitrite oxidation rates were lowest in spring/early summer
270 ($\sim 24 \mu\text{mol m}^{-2} \text{d}^{-1}$) and increased between June to September ($38\text{-}45 \mu\text{mol m}^{-2} \text{d}^{-1}$) (Table 1).
271 Nitrite oxidation maxima (~ 100 m) were deeper than those of ammonia oxidation (~ 60 m),
272 which may be related to the higher sensitivity of nitrite oxidizers to light (Wan et al., 2021).
273 Our results demonstrate that ammonia and nitrite oxidation occurred at comparable rates, which
274 is consistent with the typically low concentrations of NO_2^- observed in the GoA (Figure 1D,
275 Meeder et al., 2012).



276

277 **Figure 3:** Vertical distribution of ammonia oxidation (A,B) and nitrite oxidation (C,D) in the
 278 upper euphotic zone in the GoA, N Red Sea between May and September 2023. The Box
 279 Wisker plots sum the data distribution per depth (n=5).

280

281 3.3 Contribution of ammonia and nitrite oxidation to DCF

282 DCF is widely thought to be dominated by ammonia and nitrite oxidation, as these
 283 metabolic processes provide energy that, in turn, support chemoautotrophic CO₂ assimilation
 284 (Middelburg, 2011). While other chemoautotrophic metabolisms, such as sulfur oxidation,
 285 anammox or methanotrophy also represent important drivers of chemoautotrophy in some
 286 environments, these are unlikely to be relevant in the oxic, oligotrophic waters of the GoA.
 287 DCF and nitrification are rarely measured simultaneously, which prevents robust assessment
 288 of this relationship. To this end, we explored DCF under the warm, high-light, nutrient-poor
 289 conditions found in the GoA (Figure 1) and how it relates to corresponding rates of nitrification



290 over the euphotic zone. We calculated the contribution of ammonia and nitrite oxidation to
291 DCF assuming 0.3 moles of C fixed per mole of NH_4^+ (Santoro et al., 2010). Overall, the depth-
292 integrated contribution of ammonia oxidation to DCF ranged between 0-2%, consistent, yet
293 often lower than reports from other oceanographic settings (Table 1). For example ammonia
294 oxidizers contributed only a small fraction to DCF in the eastern tropical Pacific, accounting
295 for <20% of depth-integrated rates (Bayer et al., 2024). The depth-integrated contribution of
296 nitrite oxidation to DCF was negligible, accounting for 0.05-0.13%. (Table 1). Thus, ammonia
297 and nitrite oxidation together could account for only ~1% of the DCF, lower than recent
298 estimates from the eastern tropical Pacific (Bayer et al., 2024), though similar to observations
299 in culture experiments with ammonia oxidizers (Bayer et al., 2023). It is notable, however, that
300 relevant conversion factors between moles C fixed per mole of N oxidized in the ocean should
301 be better constrained (and may be site-specific) (Tang et al., 2023), which could alter the
302 calculated contribution discussed here. Nevertheless, we show that ammonia and nitrite
303 oxidation link N recycling with inorganic carbon assimilation in the euphotic zone in the GoA,
304 and while their contribution to total primary production is relatively small (e.g., Figure 2), it
305 may sustain part of the microbial metabolism in the nutrient-depleted surface waters of the
306 GoA. Our results also suggest that other microbial metabolism processes (e.g., anaplerosis)
307 may also contribute to DCF in the GoA's euphotic zone and should be estimated separately in
308 future studies.

309

310 **3.4 Environmental divers affecting ammonium and nitrite oxidation**

311 Nitrification is known to be affected by PAR, oxygen levels, temperature, nitrogen
312 substrate availability, pH, as well as by other environmental factors (Ward, 2008). Our results
313 are consistent overall with previous observations at other sites as both ammonium and nitrite
314 oxidation rates linearly correlate with most of these environmental variables, either positively
315 or negatively (Figure 4). Most notably, ammonium and nitrite oxidation rates correlated with
316 increasing depth and decreasing PAR level, consistent with previous reports showing that light
317 has generally been found to inhibit nitrifier growth and nitrification rates (Merbt et al., 2012;
318 Olsen, 1989; Xu et al., 2019). Surprisingly, temperature correlated negatively with ammonium
319 and nitrite oxidation rates (Figure 4). Previous studies showed that increasing temperature
320 generally stimulates nitrification by simultaneously altering substrate availability and enzyme
321 kinetics. As temperature increases, the pKa of the NH_4^+ - NH_3 system decreases, shifting the
322 equilibrium toward NH_3 , the putative substrate of ammonia monooxygenase (Emerson et al.,
323 1975). In parallel, warming enhances enzymatic activity, accelerating the catalytic steps of both



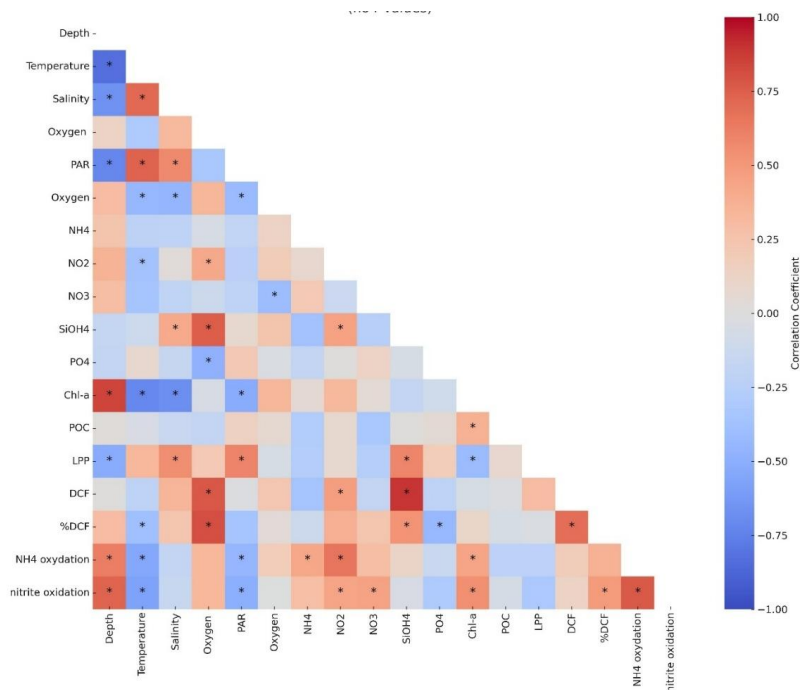
324 ammonia and nitrite oxidation (Zheng et al., 2017, 2020). We surmise that in the stratified GoA,
325 warming strengthened stratification, enhanced photoinhibition, and thereby increased
326 biological competition for ammonium, thus reducing substrate supply to nitrifiers despite
327 favorable enzyme kinetics, leading to the observed negative correlation between temperature
328 and nitrification. In agreement with this line of thought, substrate availability was positively
329 correlated with ammonia oxidation (NH_4^+ , NO_2^-) and nitrite oxidation (NO_2^- , NO_3^-),
330 highlighting the substrate-dependent nature of nitrification. Ammonia oxidation requires NH_4^+
331 or NH_3 as the electron donor, while nitrite oxidation depends on NO_2^- availability. Elevated
332 ambient concentrations of these substrates make them more available to nitrifying enzymes,
333 resulting in higher reaction rates until enzymatic saturation or co-limitation with other nutrients
334 are reached (e.g., trace metal, PO_4^+). In oligotrophic systems such as the GoA, where ambient
335 NH_4^+ and NO_2^- concentrations are exceptionally low, even small pulses of reduced or
336 intermediate nitrogen (e.g., from organic matter remineralization, mixing, or atmospheric
337 deposition) may trigger an increase in nitrification rates.

338 Nitrification is generally expected to show a negative relationship with chlorophyll.*a*
339 in surface waters, where phytoplankton may compete with nitrifiers for reduced nitrogen
340 species. Consequently, most studies report suppressed ammonium and nitrite oxidation rates
341 near the surface and enhanced rates below the chlorophyll maximum once light levels decrease
342 and substrate regeneration through organic matter remineralization becomes more important
343 (Beman et al., 2013; Yool et al., 2007). Here, however, we observed a positive correlation
344 between chlorophyll.*a* and ammonium or nitrite oxidation (as well as with photosynthesis,
345 although not significantly). This trend can be explained by the deep setting of the chlorophyll
346 maximum (~80-100 m), where phytoplankton biomass is relatively high, but light is low and
347 organic matter turnover is high, potentially providing regenerated NH_4^+ that fuels nitrification.
348 These findings suggest that the expected negative coupling at the surface is offset by strong
349 regeneration and oxidation processes near the deep chlorophyll maxima, resulting in an overall
350 positive relationship when integrated across the euphotic zone.

351 We expected that ammonium and nitrite oxidation would show a significant correlation
352 with DCF (see discussion above). Nevertheless, although both ammonium and nitrite oxidation
353 were positively coupled with DCF, the correlations were not statistically significant and is in
354 line with the overall low contribution of these processes to DCF (discussion above and see
355 Table 1). This suggests that additional pathways such as anaplerotic processes may contribute
356 to DCF (Dijkhuizen and Harder, 1984; Erb, 2011), while the contribution of ammonium and
357 nitrite oxidation to total DCF is low (Table 1).



358



359

360 **Figure 4:** A heatmap showing Pearson correlation coefficients among measured environmental
 361 parameters and biogeochemical rates. Color shading indicates the strength and direction of the
 362 correlation. Asterisks denote statistically significant correlations ($p < 0.05$).

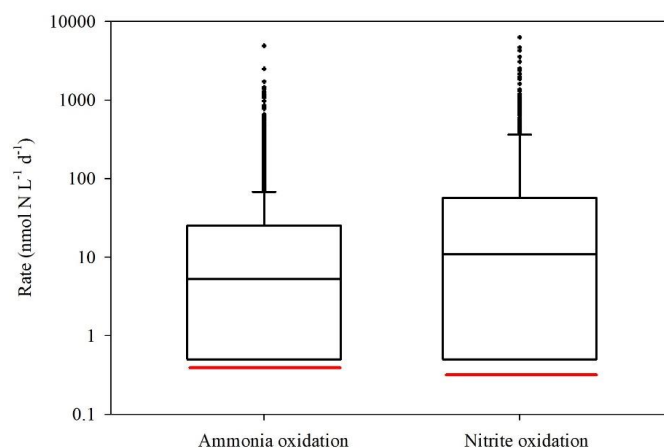
363

364 4 Conclusions

365 Globally, ammonium and nitrite oxidation rates in the euphotic zone span several orders
 366 of magnitude across oceanic environments (Figure 5). The rates we measured in the GoA
 367 during summer fall below these global medians (i.e., the red vs. black lines in Figure 5). The
 368 reason for the low rates in GoA is attributed to the low substrate availability during summertime
 369 (Figure 1C-E). The combination of high light intensity (Figure 1B) and penetration (i.e., $K_d \approx$
 370 0.04 m^{-1}) and enhanced stratification (Figure 1A) can further suppress nitrifier activity, either
 371 through photoinhibition of ammonia monooxygenase and/or by pushing microbial
 372 communities closer to their thermal tolerance limits. Our results emphasize that global
 373 compilations may be skewed toward more productive systems/seasons, and that nitrification in
 374 extremely nutrient-depleted regions may operate at lower rates and is tightly coupled to local
 375 nitrogen cycling.



376 Future studies should focus on resolving the temporal and spatial variability of
377 nitrification rates and nitrifier communities in the context of ongoing climate change. This is
378 especially true for the GoA that experience rapid warming and ocean acidification. Long-term
379 time series and diel-scale observations are needed to capture seasonal, interannual, and daily
380 dynamics, particularly in relation to stratification, warming, and nutrient supply. Advanced
381 molecular approaches such as metagenomics, metatranscriptomics, and single-cell tools should
382 be applied to link community composition and functional potential with *in-situ* rate
383 measurements. Parallel measurements of trace metals will be essential to assess their role as
384 cofactors or inhibitors of key enzymes in ammonium and nitrite oxidation. Ultimately,
385 combining high-resolution field observations with targeted manipulations and modelling will
386 improve our ability to predict how nitrification responds to environmental change and
387 contributes to current and future ocean nitrogen cycling.



388

389 **Figure 5:** A literature compilation of reported euphotic zone's ammonia oxidation and nitrite
390 oxidation recently reviewed Tang et al., (2023) and this study. The black line inside the boxes
391 shows the median value of all studies considered, while the red line indicates the median
392 values measured in the GoA during this study.

393

394 *Data availability.* All the data is presented in the graphs/table/text and will be made available
395 in excel format upon request.

396 *Author contributions.* Conceptualized and conducted the field measurements; ER. Data
397 curation, formal analysis, and visualization; ER, SDW and AP. The paper was prepared by ER,
398 SDW and AP.



399 *Competing interests.* The contact author has declared that none of the authors has any
400 competing interests.

401 *Acknowledgments.* The authors thank the personnel in the Inter University Institute for Marine
402 Sciences in Eilat (IUI). This paper was supported by a grant from the Middle East Regional
403 Cooperation (MERC) (M39-011) to ER and AP.

404

405 **References**

406 Ali, M., Balala, A. C., Kumar, S., Bhavya, P. S., and Wafar, M.: Primary production in the
407 northern Red Sea, *J. Mar. Syst.*, 132, 75–82, <https://doi.org/10.1016/j.jmarsys.2014.01.006>,
408 2014.

409 Badran, M. I., Rasheed, M., Manasrah, R., Al-najjar, T., Station, M. S., and Faculty, V.:
410 Nutrient flux fuels the summer primary productivity in the oligotrophic waters of the Gulf of
411 Aqaba, Red Sea, *Oceanologia*, 47, 47–60, 2005.

412 Bayer, B., McBeain, K., Carlson, C. A., and Santoro, A. E.: Carbon content, carbon fixation
413 yield and dissolved organic carbon release from diverse marine nitrifiers, *Limnol. Oceanogr.*,
414 68, 84–96, <https://doi.org/https://doi.org/10.1002/lno.12252>, 2023.

415 Bayer, B., Kitzinger, K., Paul, N. L., Albers, J. B., Saito, M. A., Carlson, C. A., and Santoro,
416 A. E.: Contribution of ammonia oxidizers to inorganic carbon fixation in the dark ocean,
417 *bioRxiv*, <https://doi.org/10.1101/2024.11.16.623942>, 2024.

418 Bayer, B., Kitzinger, K., Paul, N. L., Albers, J. B., Saito, M. A., Wagner, M., Carlson, C. A.,
419 and Santoro, A. E.: Bayer 2025.pdf, *Nat. Geosci.*, 18, 1144–1151, 2025.

420 Beman, J. M., Chow, C.-E., King, A. L., Feng, Y., Fuhrman, J. A., Andersson, A., Bates, N.
421 R., Popp, B. N., and Hutchins, D. A.: Global declines in oceanic nitrification rates as a
422 consequence of ocean acidification, *Proc. Natl. Acad. Sci.*, 108, 208–213,
423 <https://doi.org/10.1073/pnas.1011053108>, 2011.

424 Beman, J. M., Leilei Shih, J., and Popp, B. N.: Nitrite oxidation in the upper water column
425 and oxygen minimum zone of the eastern tropical North Pacific Ocean, *ISME J.*, 7, 2192–
426 2205, <https://doi.org/10.1038/ismej.2013.96>, 2013.

427 Berman-Frank, I. and Rahav, E.: Nitrogen fixation as a source for new production in the
428 Mediterranean Sea: a review, in: *Life in the Mediterranean Sea: A Look at Habitat Changes*,
429 Nova Science Publishers, NY, 199–226, 2012.

430 Bristow, L. A., Sarode, N., Cartee, J., Caro-Quintero, A., Thamdrup, B., and Stewart, F. J.:
431 Biogeochemical and metagenomic analysis of nitrite accumulation in the Gulf of Mexico
432 hypoxic zone, *Limnol. Oceanogr.*, 60, 1733–1750,
433 <https://doi.org/https://doi.org/10.1002/lno.10130>, 2015.

434 Chen, Y., Paytan, A., Chase, Z., Measures, C., Beck, A. J., Sañudo-Wilhelmy, S. A., and
435 Post, A. F.: Sources and fluxes of atmospheric trace elements to the Gulf of Aqaba, Red Sea,
436 *J. Geophys. Res. Atmos.*, 113, 1–13, <https://doi.org/10.1029/2007JD009110>, 2008.

437 Clark, D. R., Rees, A. P., and Joint, I.: Ammonium regeneration and nitrification rates in the
438 oligotrophic Atlantic Ocean: Implications for new production estimates, *Limnol. Oceanogr.*,



- 439 53, 52–62, <https://doi.org/https://doi.org/10.4319/lo.2008.53.1.0052>, 2008.
- 440 Clark, D. R., Rees, A. P., Ferrera, C. M., Al-moosawi, L., Somerfield, P. J., Harris, C.,
441 Quartly, G. D., Goult, S., Tarran, G., and Lessin, G.: Nitrite regeneration in the oligotrophic
442 Atlantic Ocean, *Biogeosciences*, 19, 1355–1376, [https://doi.org/https://doi.org/10.5194/bg-](https://doi.org/https://doi.org/10.5194/bg-19-1355-2022)
443 19-1355-2022, 2022.
- 444 Daims, H., Lebedeva, E. V., Pjevac, P., Han, P., Herbold, C., Albertsen, M., Jehmlich, N.,
445 Palatinszky, M., Vierheilig, J., Bulaev, A., Kirkegaard, R. H., von Bergen, M., Rattei, T.,
446 Bendinger, B., Nielsen, P. H., and Wagner, M.: Complete nitrification by *Nitrospira* bacteria,
447 *Nature*, 528, 504–509, <https://doi.org/10.1038/nature16461>, 2015.
- 448 Dijkhuizen, L. and Harder, W.: Current views on the regulation of autotrophic carbon dioxide
449 fixation via the Calvin cycle in bacteria, *Antonie Van Leeuwenhoek*, 50, 473–487, 1984.
- 450 Dishon, G., Dubinsky, Z., Caras, T., Rahav, E., Bar-Zeev, E., Tzuber, Y., and Iluz, D.:
451 Optical habitats of ultraphytoplankton groups in the Gulf of Eilat (Aqaba), Northern Red Sea,
452 *Int. J. Remote Sens.*, 33, 2683–2705, <https://doi.org/10.1080/01431161.2011.619209>, 2012.
- 453 Emerson, K., Russo, R. C., Lund, R. E., and Thurston, R. V: Aqueous ammonia equilibrium
454 calculations: effect of pH and temperature, *J. Fish. Res. Board Canada*, 32, 2379–2383,
455 <https://doi.org/10.1139/f75-274>, 1975.
- 456 Eppley, R. W. and Peterson, B. J.: Particulate organic matter flux and planktonic new
457 production in the deep ocean, *Nature*, 282, 677–680, <https://doi.org/10.1038/282677a0>, 1979.
- 458 Erb, T. J.: Carboxylases in natural and synthetic microbial pathways,
459 <https://doi.org/10.1128/AEM.05702-11>, December 2011.
- 460 Fawcett, S. E., Lomas, M. W., Casey, J. R., Ward, B. B., and Sigman, D. M.: Assimilation of
461 upwelled nitrate by small eukaryotes in the Sargasso Sea, *Nat. Geosci.*, 4, 717–722,
462 <https://doi.org/10.1038/ngeo1265>, 2011.
- 463 Fei, X., Jian-Gong, W., Ting, Z., Bin, Z., Sung-Keun, R., and Zhe-Xue, Q.: Ubiquity and
464 diversity of complete ammonia oxidizers (Comammox), *Appl. Environ. Microbiol.*, 84,
465 e01390-18, <https://doi.org/10.1128/AEM.01390-18>, 2018.
- 466 Francis, C. A., Roberts, K. J., Beman, J. M., Santoro, A. E., and Oakley, B. B.: Ubiquity and
467 diversity of ammonia-oxidizing archaea in water columns and sediments of the ocean, *Proc.*
468 *Natl. Acad. Sci.*, 102, 14683–14688, <https://doi.org/10.1073/pnas.0506625102>, 2005.
- 469 Fuller, N. J., West, N. J., Marie, D., Yallop, M., Rivlin, T., Post, A. F., Interuniversity, T.,
470 Sciences, M., Beach, C., and Scanlan, D. J.: Dynamics of community structure and phosphate
471 status of picocyanobacterial populations in the Gulf of Aqaba, *Red Sea*, 50, 363–375, 2005.
- 472 Grasshoff, K., Kremling, K., and Ehrhardt, M.: *Methods of seawater analysis*, 3rd ed., edited
473 by: Kremling, K., Ehrenreich, I. M., and Grasshoff, K., Wiley, New York, 632 pp., 1999.
- 474 Henriksen, K. and Kemp, W. M.: Nitrification in estuarine and coastal marine sediments, in:
475 *Nitrogen Cycling in Coastal Marine Environments*, edited by: Blackburn, T. . and Sorensen,
476 J., John Wiley & Sons, Ltd, 207–249, 1988.
- 477 Herbert, R. A.: Nitrogen cycling in coastal marine ecosystems, *FEMS Microbiol. Rev.*, 23,
478 563–590, <https://doi.org/10.1111/j.1574-6976.1999.tb00414.x>, 1999.
- 479 Holms, R. ., Aminot, A., K erouel, R., Hooker, B. ., and Peterson, B. .: A simple and precise



- 480 method for measuring ammonium in marine and freshwater ecosystems, *Can. Data Rep. Fish.*
481 *Aquat. Sci.*, 56, 1801–1808, <https://doi.org/10.1139/cjfas-56-10-1801>, 1999.
- 482 van Kessel, M. A. H. J., Speth, D. R., Albertsen, M., Nielsen, P. H., Op den Camp, H. J. M.,
483 Kartal, B., Jetten, M. S. M., and Lücker, S.: Complete nitrification by a single
484 microorganism, *Nature*, 528, 555–559, <https://doi.org/10.1038/nature16459>, 2015.
- 485 Ko, E., Gorbunov, M. Y., Jung, J., Lee, Y., Cho, K., Yang, E. J., and Park, J.: Phytoplankton
486 photophysiology varies depending on nitrogen and light availability at the subsurface
487 chlorophyll maximum in the northern Chukchi Sea, *Front. Mar. Sci.*, 979998,
488 <https://doi.org/10.3389/fmars.2022.979998>, 2022.
- 489 Mackey, K. R. M., Labiosa, R. G., Calhoun, M., Street, J. H., Post, A. F., and Paytan, A.:
490 Phosphorus availability, phytoplankton community dynamics, and taxon-specific phosphorus
491 status in the Gulf of Aqaba, Red Sea, *Limnol. Oceanogr.*, 52, 873–885,
492 <https://doi.org/10.4319/lo.2007.52.2.0873>, 2007.
- 493 Mackey, K. R. M., Bristow, L., Parks, D. R., Altabet, M. A., Post, A. F., and Paytan, A.: The
494 influence of light on nitrogen cycling and the primary nitrite maximum in a seasonally
495 stratified sea, *Prog. Oceanogr.*, 91, 545–560,
496 <https://doi.org/https://doi.org/10.1016/j.pocean.2011.09.001>, 2011.
- 497 Martocello, D. E. and Wankel, S. D.: Physiological influence of Fe and Cu availability on
498 nitrogen isotope fractionation during ammonia oxidation, *Environ. Sci. Technol.*, 58, 421–
499 431, <https://doi.org/10.1021/acs.est.3c05964>, 2024.
- 500 McIlvin, M. R. and Altabet, M. A.: Chemical conversion of nitrate and nitrite to nitrous oxide
501 for nitrogen and oxygen isotopic analysis in freshwater and seawater, *Anal. Chem.*, 77, 5589–
502 5595, <https://doi.org/10.1021/ac050528s>, 2005.
- 503 Mduyana, M., Thomalla, S. J., Philibert, R., Ward, B. B., and Fawcett, S. E.: The seasonal
504 cycle of nitrogen uptake and nitrification in the Atlantic sector of the Southern Ocean, *Global*
505 *Biogeochem. Cycles*, 34, e2019GB006363,
506 <https://doi.org/https://doi.org/10.1029/2019GB006363>, 2020.
- 507 Meeder, E., MacKey, K. R. M., Paytan, A., Shaked, Y., Iluz, D., Stambler, N., Rivlin, T.,
508 Post, A. F., and Lazar, B.: Nitrite dynamics in the open ocean-clues from seasonal and
509 diurnal variations, *Mar. Ecol. Prog. Ser.*, 453, 11–26, <https://doi.org/10.3354/meps09525>,
510 2012.
- 511 Merbt, S. N., Stahl, D. A., Casamayor, E. O., Martí, E., Nicol, G. W., and Prosser, J. I.:
512 Differential photoinhibition of bacterial and archaeal ammonia oxidation, *FEMS Microbiol.*
513 *Let.*, 327, 41–46, <https://doi.org/10.1111/j.1574-6968.2011.02457.x>, 2012.
- 514 Mescioglou, E., Rahav, E., Frada, M. J., Rosenfeld, S., Raveh, O., Galletti, Y., Santinelli, C.,
515 Herut, B., and Paytan, A.: Dust-associated airborne microbes affect primary and bacterial
516 production rates, and eukaryotes diversity, in the Northern Red Sea: A mesocosm approach,
517 *Atmosphere (Basel)*, 10, <https://doi.org/10.3390/atmos10070358>, 2019.
- 518 Middelburg, J. J.: Chemoautotrophy in the ocean, *Geophys. Res. Lett.*, 38, 94–97,
519 <https://doi.org/10.1029/2011GL049725>, 2011.
- 520 Mincer, T. J., Church, M. J., Taylor, L. T., Preston, C., Karl, D. M., and DeLong, E. F.:
521 Quantitative distribution of presumptive archaeal and bacterial nitrifiers in Monterey Bay and
522 the North Pacific Subtropical Gyre, *Environ. Microbiol.*, 9, 1162–1175,



- 523 <https://doi.org/https://doi.org/10.1111/j.1462-2920.2007.01239.x>, 2007.
- 524 Moutin, T. and Raimbault, P.: Primary production, carbon export and nutrients availability in
525 western and eastern Mediterranean Sea in early summer 1996 (MINOS cruise), *J. Mar. Syst.*,
526 33–34, 273–288, [https://doi.org/10.1016/S0924-7963\(02\)00062-3](https://doi.org/10.1016/S0924-7963(02)00062-3), 2002.
- 527 Olsen, R.: Differential photoinhibition of marine nitrifying bacteria: a possible mechanism
528 for the formation of the primary nitrite maximum, *J. Mar. Syst.*, 31, 227–238, 1989.
- 529 Pachiadaki, M. G., Sintes, E., Bergauer, K., Brown, J. M., Record, N. R., Swan, B. K.,
530 Mathyer, M. E., Hallam, S. J., Lopez-Garcia, P., Takaki, Y., Nunoura, T., Woyke, T., Herndl,
531 G. J., and Stepanauskas, R.: Major role of nitrite-oxidizing bacteria in dark ocean carbon
532 fixation, *Science (80-.)*, 358, 1046–1051, <https://doi.org/10.1126/science.aan8260>, 2017.
- 533 Rahav, E., Herut, B., Mulholland, M. R., Belkin, N., Elifantz, H., and Berman-frank, I.:
534 Heterotrophic and autotrophic contribution to dinitrogen fixation in the Gulf of Aqaba, *Mar.*
535 *Ecol. Prog. Ser.*, 522, 67–77, <https://doi.org/10.3354/meps11143>, 2015.
- 536 Reich, T., Belkin, N., Sisma-Ventura, G., Berman-Frank, I., and Rahav, E.: Significant dark
537 inorganic carbon fixation in the euphotic zone of an oligotrophic sea, *Limnol. Oceanogr.*,
538 9999, 1–14, <https://doi.org/10.1002/lno.12560>, 2024.
- 539 Reich, T., Belkin, N., Sisma-ventura, G., Hauzer, H., Berman-frank, I., and Rahav, E.: Does
540 oligotrophy favor chemoautotrophy over photoautotrophy ?, *Prog. Oceanogr.*, 241, 103633,
541 <https://doi.org/10.1016/j.pocean.2025.103633>, 2026.
- 542 Santoro, A. E., Casciotti, K. L., and Francis, C. A.: Activity, abundance and diversity of
543 nitrifying archaea and bacteria in the central California current, *Environ. Microbiol.*, 12,
544 1989–2006, <https://doi.org/https://doi.org/10.1111/j.1462-2920.2010.02205.x>, 2010.
- 545 Shafiee, R. T., Snow, J. T., Zhang, Q., and Rickaby, R. E. M.: Iron requirements and uptake
546 strategies of the globally abundant marine ammonia-oxidising archaeon, *Nitrosopumilus*
547 *maritimus* SCM1, *ISME J.*, 13, 2295–2305, <https://doi.org/10.1038/s41396-019-0434-8>,
548 2019.
- 549 Shafiee, R. T., Diver, P. J., Snow, J. T., Zhang, Q., and Rickaby, R. E. M.: Marine ammonia-
550 oxidising archaea and bacteria occupy distinct iron and copper niches, *ISME Commun.*, 1, 1,
551 <https://doi.org/10.1038/s43705-021-00001-7>, 2021.
- 552 Shiozaki, T., Ijichi, M., Fujiwara, A., Makabe, A., Nishino, S., Yoshikawa, C., and Harada,
553 N.: Factors regulating nitrification in the Arctic Ocean: potential impact of sea ice reduction
554 and ocean acidification, *Global Biogeochem. Cycles*, 33, 1085–1099,
555 <https://doi.org/https://doi.org/10.1029/2018GB006068>, 2019.
- 556 Sigman, D. M., Casciotti, K. L., Andreani, M., Barford, C., Galanter, M., and Böhlke, J. K.:
557 A bacterial method for the nitrogen isotopic analysis of nitrate in seawater and freshwater,
558 *Anal. Chem.*, 73, 4145–4153, <https://doi.org/10.1021/ac010088e>, 2001.
- 559 Stambler, N.: Light and picophytoplankton in the Gulf of Eilat (Aqaba), *J. Geophys. Res.*,
560 111, C11009, 2006.
- 561 Stambler, N.: Underwater light field of the Mediterranean Sea, in: *Life in the Mediterranean*
562 *Sea: A Look at Habitat Changes*, edited by: Stambler, N., Nova Science Publishers, 1–739,
563 2012.
- 564 Steemann-Nielsen, E.: The use of radioactive carbon (^{14}C) for measuring organic production



- 565 in the sea, *J. des Cons. Int. Pour Explor. la Mer*, 18, 117–140, 1952.
- 566 Suggett, D. J., Stambler, N., Prášil, O., Kolber, Z., Quigg, A., Vázquez-Dominguez, E.,
567 Zohary, T., Berman, T., Iluz, D., Levitan, O., Lawson, T., Meeder, E., Lazar, B., Bar-Zeev,
568 E., Medova, H., and Berman-Frank, I.: Nitrogen and phosphorus limitation of oceanic
569 microbial growth during spring in the Gulf of Aqaba, *Aquat. Microb. Ecol.*, 56, 227–239,
570 2009.
- 571 Tang, W., Ward, B. B., Beman, M., Bristow, L., Clark, D., Fawcett, S., Frey, C., Fripiat, F.,
572 Herndl, G. J., Mduyana, M., Paulot, F., Peng, X., Santoro, A. E., Shiozaki, T., Sintès, E.,
573 Stock, C., Sun, X., Wan, X. S., Xu, M. N., and Zhang, Y.: Database of nitrification and
574 nitrifiers in the global ocean, *Earth Sci. Rev.*, 15, 5039–5077,
575 <https://doi.org/https://doi.org/10.5194/essd-15-5039-2023>, 2023.
- 576 Torfstein, A., Teutsch, N., Tirosch, O., Shaked, Y., Rivlin, T., Zipori, A., Stein, M., Lazar, B.,
577 and Erel, Y.: Chemical characterization of atmospheric dust from a weekly time series in the
578 north Red Sea between 2006 and 2010, *Geochim. Cosmochim. Acta*, 211, 373–393,
579 <https://doi.org/10.1016/j.gca.2017.06.007>, 2017.
- 580 Wan, X. S., Sheng, H.-X., Dai, M., Church, M. J., Zou, W., Li, X., Hutchins, D. A., Ward, B.
581 B., and Kao, S.-J.: Phytoplankton-nitrifier interactions control the geographic distribution of
582 nitrite in the upper ocean, *Global Biogeochem. Cycles*, 35, e2021GB007072,
583 <https://doi.org/https://doi.org/10.1029/2021GB007072>, 2021.
- 584 Wankel, S. D., Kendall, C., Pennington, J. T., Chavez, F. P., and Paytan, A.: Nitrification in
585 the euphotic zone as evidenced by nitrate dual isotopic composition: Observations from
586 Monterey Bay, California, *Glob. Biochem. cycles*, 21, 1–13,
587 <https://doi.org/10.1029/2006GB002723>, 2007.
- 588 Ward, B. B.: Nitrogen transformations in the Southern California Bight, *Deep Sea Res. Part*
589 *A. Oceanogr. Res. Pap.*, 34, 785–805, [https://doi.org/https://doi.org/10.1016/0198-](https://doi.org/https://doi.org/10.1016/0198-0149(87)90037-9)
590 [0149\(87\)90037-9](https://doi.org/https://doi.org/10.1016/0198-0149(87)90037-9), 1987.
- 591 Ward, B. B.: Nitrification in Marine Systems, in: *Nitrogen in the Marine Environment*
592 *Environment*, edited by: Capon, D. G., Bronk, D. A., Mulholland, M. R., and Carpenter, E.
593 J., Elsevier, 199–262, <https://doi.org/10.1016/B978-0-12-372522-6.00005-0>, 2008.
- 594 Welschmeyer, N. A.: Fluorometric analysis of chlorophyll a in the presence of chlorophyll b
595 and pheopigments, *Limnol. Oceanogr.*, 39, 1985–1992, 1994.
- 596 Wuchter, C., Abbas, B., Coolen, M. J. L., Herfort, L., van Bleijswijk, J., Timmers, P., Strous,
597 M., Teira, E., Herndl, G. J., Middelburg, J. J., Schouten, S., and Sinninghe Damsté, J. S.:
598 Archaeal nitrification in the ocean, *Proc. Natl. Acad. Sci.*, 103, 12317–12322,
599 <https://doi.org/10.1073/pnas.0600756103>, 2006.
- 600 Xu, M. N., Li, X., Shi, D., Zhang, Y., Dai, M., Huang, T., Glibert, P. M., and Kao, S.-J.:
601 Coupled effect of substrate and light on assimilation and oxidation of regenerated nitrogen in
602 the euphotic ocean, *Limnol. Oceanogr.*, 64, 1270–1283,
603 <https://doi.org/https://doi.org/10.1002/lno.11114>, 2019.
- 604 Yool, A., Martin, A. P., Fernández, C., and Clark, D. R.: The significance of nitrification for
605 oceanic new production, *Nature*, 447, 999–1002, <https://doi.org/10.1038/nature05885>, 2007.
- 606 Zheng, Z.-Z., Wan, X., Xu, M. N., Hsiao, S. S.-Y., Zhang, Y., Zheng, L.-W., Wu, Y., Zou,
607 W., and Kao, S.-J.: Effects of temperature and particles on nitrification in a eutrophic coastal



- 608 bay in southern China, *J. Geophys. Res. Biogeosciences*, 122, 2325–2337,
609 <https://doi.org/https://doi.org/10.1002/2017JG003871>, 2017.
- 610 Zheng, Z.-Z., Zheng, L.-W., Xu, M. N., Tan, E., Hutchins, D. A., Deng, W., Zhang, Y., Shi,
611 D., Dai, M., and Kao, S.-J.: Substrate regulation leads to differential responses of microbial
612 ammonia-oxidizing communities to ocean warming, *Nat. Commun.*, 11, 3511,
613 <https://doi.org/10.1038/s41467-020-17366-3>, 2020.
- 614 Zhu, W., Wang, C., Hill, J., He, Y., Tao, B., Mao, Z., and Wu, W.: A missing link in the
615 estuarine nitrogen cycle? Coupled nitrification-denitrification mediated by suspended
616 particulate matter, *Sci. Rep.*, 8, 2282, <https://doi.org/10.1038/s41598-018-20688-4>, 2018.